Outage Probability Analysis of STAR-RIS Assisted NOMA Network with Correlated Channels

Tianxiong Wang, Mihai-Alin Badiu, Gaojie Chen, *Senior Member, IEEE,*
and Justin P. Coon, *Senior Member, IEEE*

***Abstract*—In this paper, we investigate the outage probability of a simultaneously transmitting and reflecting reconfigurable intelligent surface (STAR-RIS) assisted downlink non-orthogonal multiple access (NOMA) network over spatially correlated channels. To evaluate the impact of channel correlations on the system performance, we first approximate the distribution of the composite channel gain as a gamma random variable via a moment-matching approach and then derive new close-form outage probability expressions for a pair of NOMA users. Based on the approximate results, the diversity of each user is studied. Numerical results are provided to validate the effectiveness of the theoretical analysis and illustrate the performance loss due to channel correlations.**

***Index Terms*—Reconfigurable intelligent surface, NOMA, channel correlation, simultaneous transmission and reflection**

I. Introduction

Reconfigurable Intelligent surfaces (RISs) have been considered as a revolutionary physical layer technique in the future wireless communication network [1]. Physically, a RIS consists of massive reflecting elements, which can reconfigure the wireless environment by adjusting the electromagnetic response of each reflecting element. Compared to multiple-input multiple-output (MIMO) and relay systems, a RIS does not utilize the costly and energy-consuming radio frequency chains, which makes RIS an energy-efficient and economical technique for future wireless networks [2].

Despite the benefits mentioned above, a problem of RIS is that the conventional reflecting-only RIS requires that receivers and transmitters need to locate at the same side, which significantly limits the service coverage. To tackle this problem, a new technique of simultaneously transmitting and reflecting reconfigurable intelligent surface (STAR-RIS) was investigated recently. Compared with the reflecting RIS, a STAR-RIS is able to transmit and reflect the impinging waves to receivers located at different sides of the surface. A STAR-RIS prototype was designed by NTT DOCOMO in Japan [3]. Three implementation strategies of STAR-RIS, i.e., mode switching, energy splitting, and time switching, were presented in [4]. The authors in [5] studied the phase shift design of a STAR-RIS assisted network and showed the advantages of STAR-RIS in enlarging the coverage.

This work was supported by EPSRC grant number EP/T02612X/1.

T. Wang, M. A. Badiu and J. P. Coon are with the Department of Engineering Science, University of Oxford, Oxford, OX1 3PJ, U.K. (e-mail: {tianxiong.wang, mihai.badiu, justin.coon@eng.ox.ac.uk}@eng.ox.ac.uk).

G. Chen is with 5GIC & 6GIC, Institute for Communication Systems (ICS), University of Surrey, Guildford, GU2 7XH, United Kingdom (e-mail: gaojie.chen@surrey.ac.uk).

Due to the superiority of STAR-RIS, especially in providing full-space coverage of multiple users, STAR-RIS empowered multiple access attracts great research interests. Among various multiple access techniques, NOMA has received significant attention due to advantages over orthogonal multiple access (OMA) in terms of high spectrum efficiency, massive connectivity, and balancing user fairness [6]. A few research works focusing on the analysis of STAR-RIS assisted NOMA networks have appeared recently. The authors in [7] optimized the coverage of a STAR-RIS assisted NOMA network under the quality of service (QoS) requirement of each user. A mode switching STAR-RIS aided NOMA network was analyzed in [8], where an algorithm to partition elements was proposed to maximize the sum-rate. The authors in [9] and [10] derived the outage probability and diversity gains of a STAR-RIS empowered NOMA system with perfect and imperfect successive interference cancellation (SIC).

Most of the previous works assumed the channels associated with the STAR-RIS are independent. However, this assumption is not practical for a real system in which elements are usually placed in a rectangular array [11], [12]. The authors in [13] optimized the sum-rate of a RIS-assisted multi-user system under a correlated Rician channel model. However, the fundamental performance analysis of STAR-RIS systems over correlated channels is still at an embryonic stage. To tackle these issues, this letter is the first work to analyze the outage probability of a STAR-RIS assisted NOMA network where the channels are spatially correlated. First, approximate closed-form expressions of the outage probability are derived by using a moment-matching method. Then, the diversity of each user is investigated. Finally, numerical results show that the proposed analytical results are accurate, and channel correlations deteriorate system outage performance.

Notations: Bold lower and upper case letters represent vectors and matrices, respectively. $\mathcal{CN}(\cdot,\cdot)$ is the circularly symmetric Gaussian distribution. $\mathbb{C}^{N\times 1}$ stands for the $N\times 1$ complex vectors space. $\|\cdot\|$ is the Euclidean norm. $\mathrm{diag}(\mathbf{a})$ represents a diagonal matrix with $\mathbf{a}$ on its main diagonal. $[\mathbf{A}]_{i,j}$ is the (i,j) entry of $\mathbf{A}$. $\mathbb{E}[\cdot]$ and $\mathrm{Var}[\cdot]$ represent the expectation and variance of a random variable. $(\cdot)^T$ is the transpose and $(\cdot)^*$ is the conjugate operation. $\mathrm{mod}(\cdot,\cdot)$ and $\lfloor\cdot\rfloor$ are the modulus operation and floor function.

II. System Model

This letter focuses on a mode switching STAR-RIS assisted wireless network in which a single-antenna transmitter (TX) communicates to single-antenna users simultaneously

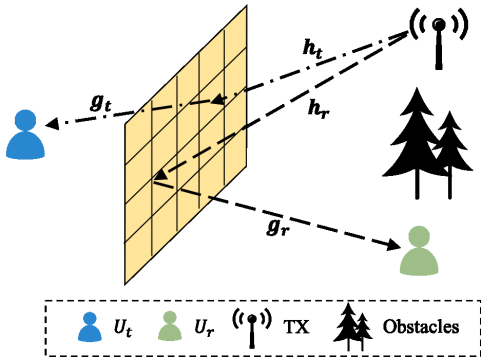

Fig. 1. System model of the STAR-RIS assisted NOMA system.

by using NOMA transmission. As shown in Fig.1, two users locate on opposite sides of the STAR-RIS. The STAR-RIS consists of $N = M_h \times M_v$ elements, with M_h elements per row and M_v elements per column. The size of each element is $A = l_0 \times w_0$, where l_0 and w_0 denote the length and width of each element. In order to serve two users simultaneously[1], the STAR-RIS elements are divided into two collections S_t and S_r with N_t and N_r elements and operating in the transmission and reflection modes, respectively. Similar to [14], it is assumed that the STAR-RIS operates in the far field of TX, U_t and U_r, and the direct links of TX-U_t and TX-U_r are blocked by obstacles. In contrast to existing works considering independent channel models, we take channel correlations into account. The normalized small scale fading of the TX-S_t and TX-S_r channels is modeled by a correlated normal random vector, i.e.,

$$\mathbf{h}_\chi \sim \mathcal{CN}(0, \mathbf{R}_\chi), \quad \chi \in \{t, r\}, \tag{1}$$

where $\mathbf{h}_\chi = \left(h_{\chi,1}, ..., h_{\chi,N_\chi}\right)^T \in \mathbb{C}^{N_\chi \times 1}$; $\mathbf{R}_\chi \in \mathbb{C}^{N_\chi \times N_\chi}$ is the covariance matrix of $\mathbf{h}_\chi$. Based on the correlation model proposed in [11], each element of $\mathbf{R}_\chi$ satisfies

$$[\mathbf{R}_\chi]_{i,j} = \text{sinc}\left(\frac{2\pi}{\lambda} \parallel \mathbf{a}_i - \mathbf{a}_j \parallel\right), \quad i, j \in \{1, ..., N_\chi\}. \tag{2}$$

where λ is the wavelength; $\parallel \mathbf{a}_i - \mathbf{a}_j \parallel$ is the distance between elements i and j. Likewise, the normalized small scale fading of the S_χ-U_χ channel is assumed to be correlated normal distributed with channel vector as

$$\mathbf{g}_\chi \sim \mathcal{CN}(0, \mathbf{R}_\chi), \quad \chi \in \{t, r\}. \tag{3}$$

The path loss coefficient of the TX-S_χ-U_χ channel is [15]

$$\eta_\chi = \frac{\Lambda_\chi A^2}{d_0^\vartheta d_\chi^\vartheta}, \quad \chi \in \{t, r\}, \tag{4}$$

where Λ_χ is the average path loss intensity at unit distance of the TX-S_χ-U_χ channel; d_0 and d_χ are the distances from TX to RIS and from RIS to U_χ, respectively; ϑ denotes the path loss exponent. The proposed channel model is suitable for urban environments with rich scatters and a stable LoS path is non-existent [16]. Since TX and users operate in the far field, $\mathbf{h}_\chi$ and $\mathbf{g}_\chi$ are independent of each other.

As per the mode switching STAR-RIS protocol introduced in [4], the elements in S_t and S_r operate in the transmission and reflection modes, respectively[2]. To be specific, for transmission mode, the incident signals penetrate the elements in S_t without reflection. The transmitting coefficients matrix is given as $\mathbf{\Theta} = \text{diag}\left(e^{j\theta_1}, ..., e^{j\theta_{N_t}}\right)$. For reflection mode, the incident signals are reflected by the elements in S_r without power loss and the reflecting coefficients matrix can be written as $\mathbf{\Psi} = \text{diag}\left(e^{j\psi_1}, ..., e^{j\psi_{N_r}}\right)$. Without loss of generality, each element is assumed to be ideal without energy consumption and the amplitude coefficient is one [8], [9].

In the proposed system, TX broadcasts the superimposed signals of U_t and U_r. As proved in [9], the received SNR of both users is maximized when a coherent phase shifting scheme is performed[3]. After the coherent phase shifting, the received signals at U_t and U_r can be expressed as

$$y_t = \sqrt{\eta_t} H_t \sqrt{P}\left(\beta_t s_t + \beta_r s_r\right) + w_t, \tag{5a}$$

$$y_r = \sqrt{\eta_r} H_r \sqrt{P}\left(\beta_t s_t + \beta_r s_r\right) + w_r, \tag{5b}$$

where $H_t = \sum_{n=1}^{N_t} |g_{t,n}||h_{t,n}|$ and $H_r = \sum_{n=1}^{N_r} |g_{r,n}||h_{r,n}|$; P is the transmit power at TX; β_t and β_r are the transmit power allocation factors for U_t and U_r at TX with $\beta_t^2 + \beta_r^2 = 1$; s_t and s_r are the signals of U_t and U_r with unit power, i.e., $\mathbb{E}[|s_t|^2] = \mathbb{E}[|s_r|^2] = 1$. w_t and w_r are the additive Gaussian noise of U_t and U_r with zero mean and variance σ_0^2.

As per the principles of NOMA, the user with a better channel condition conducts SIC, and the other user decodes its signal directly. Theoretically, the channel conditions of two users will fluctuate quickly, making the analysis of optimal decoding order complicated. In this letter, we assumed a fixed decoding order (U_r, U_t) based on the path loss[4], similar to other works [6], [9], [10], [21]. From the perspective of user fairness, more transmit power is allocated to U_r, i.e., $\beta_t < \beta_r$. In the proposed system, U_t first decodes the signal of U_r with signal to interference plus noise ratio (SINR)

$$\gamma_s = \frac{P\eta_t \beta_r^2 H_t^2}{P\eta_t \beta_t^2 H_t^2 + \sigma_0^2}. \tag{6}$$

Then, U_t subtracts the signal of U_r from its received signal and decodes its information with signal to noise ratio (SNR):

$$\gamma_t = \gamma_0 \eta_t \beta_t^2 H_t^2, \tag{7}$$

[1] In this letter, we focus on a two-user NOMA group, similarly to [9], [10]. Different NOMA groups are allocated with orthogonal resource blocks. The analysis of multi-user NOMA requires the distribution of the sum of correlated complex random variables, which remains a critical open question for our future work.

[2] Due to limited space, we only consider the mode switching STAR-RIS, same as in [8], [10]. The proposed framework can be extended to the energy splitting and time switching STAR-RIS in similar ways.

[3] In this letter, we apply ideal coherent phase shifting. Since phase errors exist in reality [17], this assumption gives a lower bound on the outage probability [18]. Further, only two-bit phase adjustment can achieve the performance close to the lower bound in practice [19], [20].

[4] In this letter, we assume $d_t < d_r$. Therefore, the path loss coefficients satisfy $\eta_t > \eta_r$. This set-up reflects the scenario where a STAR-RIS is deployed on a building to serve indoor (U_t) and outdoor (U_r) users.

where $\gamma_0 = P/\sigma_0^2$ is the transmit SNR. At the same time, U_r decodes its information by treating the signal of U_t as interference with SINR

$$\gamma_r = \frac{P\eta_r\beta_r^2 H_r^2}{P\eta_r\beta_t^2 H_r^2 + \sigma_0^2}. \tag{8}$$

III. Performance Analysis

In this section, the outage probability of the STAR-RIS assisted NOMA network is investigated. We first derive the channel distributions of H_t and H_r, based on which the outage probability expressions of U_t and U_r are obtained. With these expressions, the impact of channel correlations on the diversity of each user is discussed in detail.

A. Channel Distributions Analysis

A moment-matching approach based on gamma distribution is applied to manipulate the channel distributions of H_χ, $\chi \in \{t, r\}$. First, a Proposition regarding the expectation and variance of H_χ is given as follows.

Proposition 1. *The expectation and variance of H_χ, $\chi \in \{t, r\}$ can be computed as*

$$\mathbb{E}[H_\chi] = \frac{\pi}{4} N_\chi, \tag{9a}$$

$$\mathrm{Var}[H_\chi] = \sum_{i=1}^{N_\chi}\sum_{j=1}^{N_\chi} \left(\left[\bar{\mathbf{R}}_\chi\right]_{i,j}\right)^2 - \frac{\pi^2}{16} N_\chi^2, \tag{9b}$$

where $\bar{\mathbf{R}}_\chi \triangleq \mathbb{E}[|\mathbf{h}_\chi||\mathbf{h}_\chi|^T] = \mathbb{E}[|\mathbf{g}_\chi||\mathbf{g}_\chi|^T]$.
For $i \neq j$,

$$\left[\bar{\mathbf{R}}_\chi\right]_{i,j} = \frac{\left|\left[\mathbf{R}_\chi\right]_{i,j}\right|^2 - 1}{2} K\left(\left|\left[\mathbf{R}_\chi\right]_{i,j}\right|^2\right) + E\left(\left|\left[\mathbf{R}_\chi\right]_{i,j}\right|^2\right). \tag{10}$$

For $i = j$,

$$\left[\bar{\mathbf{R}}_\chi\right]_{i,j} = 1. \tag{11}$$

$K(\cdot)$ and $E(\cdot)$ are the complete elliptic integrals of the first and second kinds, respectively.

Proof: See the Appendix A. □

Remark 1. *When the channels are uncorrelated, the channel covariance matrix $\mathbf{R}_{\chi,u}$, $\chi \in \{t, r\}$ becomes an identity matrix, such that the expectation and variance of the composite channel gain $H_{\chi,u}$ become $\mathbb{E}[H_{\chi,u}] = \pi N_\chi/4$ and $\mathrm{Var}[H_{\chi,u}] = \left(1 - \pi^2/16\right) N_\chi$; these results, which were also derived in [22], are thus a special case of Proposition 1.*

With Proposition 1, the moment-matching approach can be utilized to analyze the distribution of H_χ by matching the expectation and variance of H_χ to a gamma random variable with mean $\kappa_\chi\omega_\chi$ and variance $\kappa_\chi\omega_\chi^2$. As introduced in [22], the gamma distribution can be used to approximate complicated SNR distributions with high accuracy and tractable parameters computations. Thus, H_χ can be approximated as a gamma random variable with shape parameter κ_χ and scale parameter ω_χ:

$$\kappa_\chi = \frac{\mathbb{E}^2[H_\chi]}{\mathrm{Var}[H_\chi]}, \quad \omega_\chi = \frac{\mathrm{Var}[H_\chi]}{\mathbb{E}[H_\chi]}. \tag{12}$$

The probability density function (PDF) and cumulative distribution function (CDF) of H_χ can be approximated as

$$f_{H_\chi}(x) \approx \frac{x^{\kappa_\chi - 1}\exp\left(-\frac{x}{\omega_\chi}\right)}{\Gamma(\kappa_\chi)\,\omega_\chi^{\kappa_\chi}}, \tag{13a}$$

$$F_{H_\chi}(x) \approx \frac{1}{\Gamma(\kappa_\chi)}\gamma\left(\kappa_\chi, \frac{x}{\omega_\chi}\right), \tag{13b}$$

where $\Gamma(\cdot)$ is gamma function and $\gamma(\cdot,\cdot)$ is lower incomplete gamma function.

B. Outage Probability of U_t

According to the principle of NOMA, the outage occurs at U_t when it cannot decode the signal of U_r or its own signal, or both. Thus, the outage probability of U_t is defined as

$$P_t = 1 - \Pr\left(\gamma_s > \bar{\gamma}_s, \gamma_t > \bar{\gamma}_t\right), \tag{14}$$

where $\bar{\gamma}_s$ and $\bar{\gamma}_t$ are the SINR threshold of SIC and SNR threshold after SIC, respectively. When $\beta_r \leq \sqrt{\bar{\gamma}_s}\beta_t$, it is clear to learn that $P_t = 1$. When $\beta_r > \sqrt{\bar{\gamma}_s}\beta_t$, substituting (6) and (7) into (14), the outage probability of U_t can be given as

$$P_t = 1 - \Pr\left(H_t > \hat{\gamma}_t\right) \approx \frac{1}{\Gamma(\kappa_t)}\gamma\left(\kappa_t, \frac{\hat{\gamma}_t}{\omega_t}\right), \tag{15}$$

where

$$\hat{\gamma}_t = \max\left\{\sqrt{\frac{\bar{\gamma}_s}{\gamma_0\eta_t\left(\beta_r^2 - \bar{\gamma}_s\beta_t^2\right)}}, \sqrt{\frac{\bar{\gamma}_t}{\gamma_0\eta_t\beta_t^2}}\right\}. \tag{16}$$

C. Outage Probability of U_r

The outage will happen at U_r when its received SINR falls below a threshold. Hence, the outage probability of U_r is defined as

$$P_r = \Pr\left(\gamma_r < \bar{\gamma}_r\right), \tag{17}$$

where $\bar{\gamma}_r$ is the SINR threshold. Following the similar procedures as in the analysis of U_t, the outage probability of U_r can be studied as follows. Under the case of $\beta_r \leq \sqrt{\bar{\gamma}_r}\beta_t$, we can have $P_r = 1$. Under the case of $\beta_r > \sqrt{\bar{\gamma}_r}\beta_t$, the outage probability of U_r can be approximated as

$$P_r \approx \frac{1}{\Gamma(\kappa_r)}\gamma\left(\kappa_r, \frac{\hat{\gamma}_r}{\omega_r}\right), \tag{18}$$

where $\hat{\gamma}_r = \sqrt{\bar{\gamma}_r/(\gamma_0\eta_r\left(\beta_r^2 - \bar{\gamma}_r\beta_t^2\right))}$.

D. Diversity Analysis

The diversity is a performance metric to evaluate how fast the outage probability decreases with the transmit SNR. Conventionally, diversity refers to an asymptotic quantity as the transmit SNR goes to infinity. However, as pointed out in [23], it is of interest to analyze the diversity at finite SNR in system design. The finite-SNR diversity is defined as

$$\bar{\delta}_\chi(\gamma_0) = -\frac{\partial \log P_\chi}{\partial \log(\gamma_0)} = -\gamma_0\frac{\partial \log P_\chi}{\partial \gamma_0}, \quad \chi \in \{t, r\}. \tag{19}$$

With (15) and (18), the finite-SNR diversity of U_t and U_r can be approximated as

$$\bar{\delta}_\chi(\gamma_0) \approx \frac{\exp\left(-\frac{\xi_\chi}{\sqrt{\gamma_0}}\right)\left(\frac{\xi_\chi}{\sqrt{\gamma_0}}\right)^{\kappa_\chi}}{2\,\gamma\left(\kappa_\chi, \frac{\xi_\chi}{\sqrt{\gamma_0}}\right)}, \quad \chi \in \{t, r\}, \tag{20}$$

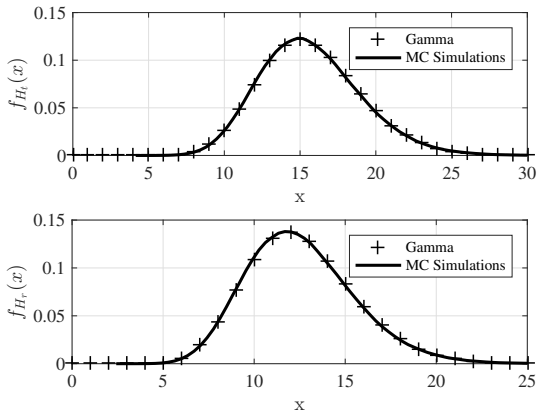

Fig. 2. Approximate PDFs of H_t and H_r and simulation results.

where

$$\xi_t = \max\left\{\sqrt{\frac{\bar{\gamma}_s}{\omega_t^2\eta_t\left(\beta_r^2-\bar{\gamma}_s\beta_t^2\right)}}, \sqrt{\frac{\bar{\gamma}_t}{\omega_t^2\eta_t\beta_t^2}}\right\}, \tag{21}$$

$$\xi_r = \sqrt{\frac{\bar{\gamma}_r}{\omega_r^2\eta_r\left(\beta_r^2-\bar{\gamma}_r\beta_t^2\right)}}. \tag{22}$$

As γ_0 goes to infinity, the conventional diversity of U_t and U_r can be approximated as

$$\delta_\chi = \lim_{\gamma_0\to\infty} \bar{\delta}_\chi(\gamma_0) \approx \frac{\kappa_\chi}{2}, \quad \chi \in \{t, r\}. \tag{23}$$

Although these are approximate results, we can still gain some insights regarding the impact of channel correlations on the outage probability. When the channels are correlated, each non-diagonal element of the channel covariance matrix satisfies $0 < |[\mathbf{R}_\chi]_{i,j}| < 1$ if $i \neq j$. Then, it can be proved that $\pi/4 < [\bar{\mathbf{R}}_\chi]_{i,j} < 1$. The variance of H_χ is rewritten as

$$\mathrm{Var}[H_\chi] = \mathrm{Var}[H_{\chi,u}] + \left(\sum_{i=1}^{N_\chi}\sum_{j=1,j\neq i}^{N_\chi}\left(\left[\bar{\mathbf{R}}_\chi\right]_{i,j}\right)^2 - \frac{\pi^2}{16}(N_\chi^2 - N_\chi)\right), \tag{24}$$

where the second term on the right hand side of (24) is larger than zero. Referring to Remark 1, the expectation and variance of the uncorrelated and correlated channel gains satisfy $\mathbb{E}[H_{\chi,u}] = \mathbb{E}[H_\chi]$, $\mathrm{Var}[H_{\chi,u}] < \mathrm{Var}[H_\chi]$. Referring to (12) and (23), we can learn that the approximate diversity of each user with correlated channels is smaller than that of uncorrelated channels. Channel correlations will deteriorate the outage performance as expected. Crucially, we have given here a quantitative description of how they do so.

IV. Numerical Results

In this section, we study the impact of channel correlations on the outage performance. The proposed analytical results are evaluated by Monte Carlo (MC) simulations. The simulation parameters are defined as follows. The SNR/SINR thresholds are $\bar{\gamma}_s = \bar{\gamma}_t = \bar{\gamma}_r = 0\,\mathrm{dB}$. The distances of the TX-RIS, RIS-U_t and RIS-U_r channels are $d_0 = 15\,\mathrm{m}$, $d_t = 8\,\mathrm{m}$ and $d_r = 15\,\mathrm{m}$, respectively. The path loss exponent is $\vartheta = 2.3$. The transmit power allocation factors are given as $\beta_t = 0.6$ and $\beta_r = 0.8$. The unit distance path loss of each element is set as $\Lambda_t A^2 = \Lambda_r A^2 = -20\,\mathrm{dB}$. The wavelength is $\lambda = 0.1\,\mathrm{m}$. The STAR-RIS element is of dimensions $l_0 = 5\,\mathrm{cm}$ and $w_0 = 3\,\mathrm{cm}$. The STAR-RIS is assumed to be partitioned into two rectangular sub-surfaces as S_χ, $\chi \in \{t, r\}$, with $M_{h,\chi}$ and $M_{v,\chi}$ elements per row and column. The element vector in (2) is given as $\mathbf{a}_\varepsilon = [0, \mathrm{mod}(\varepsilon-1, M_{h,\chi})l_0, \lfloor(\varepsilon-1)/M_{h,\chi}\rfloor w_0]$, $\varepsilon \in \{1, ..., N_\chi\}$.

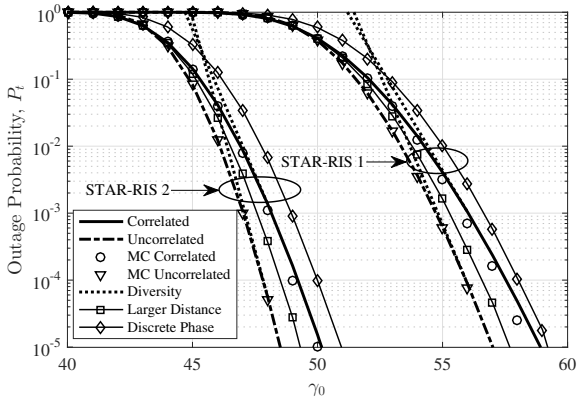

Fig. 3. Outage Probability of U_t versus γ_0. In STAR-RIS 1, $N_t = 20$; In STAR-RIS 2, $N_t = 40$.

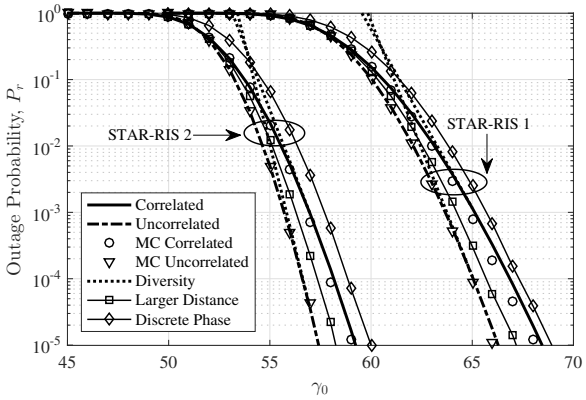

Fig. 4. Outage Probability of U_r versus γ_0. In STAR-RIS 1, $N_r = 16$; In STAR-RIS 2, $N_r = 32$.

The accuracy of gamma approximation is verified in Fig. 2. The approximate PDFs of H_t and H_r are compared with the numerical results via MC simulations. The element configuration is STAR-RIS 1: $\{N = 36; S_t : M_{h,t} = 5, M_{v,t} = 4; S_r : M_{h,r} = 4, M_{v,r} = 4\}$. As can be seen from Fig. 2, the approximate PDFs match well with the numerical results.

The outage probability of U_t and U_r versus the transmit SNR γ_0 are presented in Figs. 3 and 4, respectively. Another STAR-RIS configuration is considered: STAR-RIS 2: $\{N = 72; S_t : M_{h,t} = 5, M_{v,t} = 8; S_r : M_{h,r} = 4, M_{v,r} = 8\}$. The outage probability of U_t and U_r when the channels are assumed to be uncorrelated are given as benchmarks. Figs. 3 and 4 show that channel correlations deteriorate the outage performance. For example, when $\gamma_0 = 65\,\mathrm{dB}$

and STAR-RIS 1 is used, the outage probability of U_r is 10^{-3} and 10^{-4} for correlated and uncorrelated channels, respectively. To illustrate the impact of element spacing, we fix the element size and increase the inter-element distance by $1\,\mathrm{cm}$. The outage curves for larger element spacing are labelled 'Larger Distance'. Increasing the spacing will lead to better outage performance. We also explore the impact of channel correlations on the diversity, shown by the dotted lines with 'diversity' in the legend. For example, the finite-SNR diversity at $\gamma_0 = 56\,\mathrm{dB}$ of U_t is 6.2 and 8.9 for correlated and uncorrelated channels when STAR-RIS 1 is used. These values are much smaller than the number of elements since a finite SNR regime is studied. For a practical STAR-RIS, the asymptotic diversity slope will appear at extremely low outage probability in a very large SNR regime, which is of little engineering importance. Numerical results illustrate the diversity of each user decreases due to channel correlations. The outage probability curves with two-bit phase adjustment, labelled 'Discrete Phase', are also given. As expected, the gap between ideal and two-bit phase shifting is narrow.

V. Conclusions

This paper proposed a mode switching STAR-RIS empowered NOMA communication network over spatially correlated channels and investigated the outage probability, finite-SNR diversity and asymptotic diversity of the paired NOMA users. To be specific, the outage probability expressions were derived by using a moment-matching method based on gamma distribution and the approximate diversity of both users was then computed. It was shown that channel correlations lead to performance degradation in terms of outage probability. Numerical results confirmed the accuracy of the proposed outage expressions. An accurate asymptotic analysis of a STAR-RIS system over correlated channels constitutes an important question for further research.

Appendix A

First, the expectation of H_t can be computed directly as $\mathbb{E}[H_t] = \sum_{n=1}^{N_t} \mathbb{E}\left[|g_{t,n}|\right]\mathbb{E}\left[|h_{t,n}|\right] = \pi N_t/4$. On the other hand, the variance of H_t can be manipulated as

$$\begin{aligned}
\mathrm{Var}[H_t] &= \mathbb{E}[(H_t - \mathbb{E}[H_t])^2] \\
&= \mathbb{E}\left[\left(\sum_{n=1}^{N_t}\left(|g_{t,n}||h_{t,n}| - \mathbb{E}[|g_{t,n}||h_{t,n}|]\right)\right)^2\right] \\
&= \mathbb{E}\left[\sum_{i=1}^{N_t}\sum_{j=1}^{N_t}\left(|g_{t,i}||h_{t,i}| - \frac{\pi}{4}\right)\left(|g_{t,j}||h_{t,j}| - \frac{\pi}{4}\right)\right] \\
&= \sum_{i=1}^{N_t}\sum_{j=1}^{N_t}\left(\mathbb{E}\left[|g_{t,i}||g_{t,j}|\right]\mathbb{E}\left[|h_{t,i}||h_{t,j}|\right]\right) - \frac{\pi^2}{16}N_t^2. \qquad (25)
\end{aligned}$$

We have proved the mathematical relationship between $\mathbb{E}[|\varpi_{t,i}||\varpi_{t,j}|]$ and $\mathbb{E}[\varpi_{t,i}\varpi_{t,j}^*]$, $\varpi \in \{g, h\}$ in [20], and the relationship is given in (10) and (11), where $\mathbb{E}[|\varpi_{t,i}||\varpi_{t,j}|]$ and $\mathbb{E}[\varpi_{t,i}\varpi_{t,j}^*]$ are the (i,j) entry in matrices $\bar{\mathbf{R}}_t$ and $\mathbf{R}_t$, respectively. Exploiting (10), (11) and (25), the variance of H_t is obtained as in Proposition 1. Similarly, the expectation and variance of H_r can be obtained.

References

[1] Q. Wu and R. Zhang, "Towards smart and reconfigurable environment: Intelligent reflecting surface aided wireless network," *IEEE Commun. Mag.*, vol. 58, no. 1, pp. 106–112, 2020.

[2] Q. Wu, S. Zhang *et al.*, "Intelligent reflecting surface-aided wireless communications: A tutorial," *IEEE Trans. Commun.*, vol. 69, no. 5, pp. 3313–3351, 2021.

[3] N. DOCOMO, "Docomo conducts world's first successful trial of transparent dynamic metasurface," 2020. [Online]. Available: https://www.nttdocomo.co.jp/english/info/media_center/pr/2020/0117_00.html.

[4] Y. Liu, X. Mu *et al.*, "STAR: Simultaneous transmission and reflection for 360 coverage by intelligent surfaces," *IEEE Wireless Commun.*, vol. 28, no. 6, pp. 102–109, 2021.

[5] S. Zhang, H. Zhang *et al.*, "Beyond intelligent reflecting surfaces: Reflective-transmissive metasurface aided communications for full-dimensional coverage extension," *IEEE Trans. Veh. Technol.*, vol. 69, no. 11, pp. 13 905–13 909, 2020.

[6] Z. Chen, Z. Ding *et al.*, "On the application of quasi-degradation to MISO-NOMA downlink," *IEEE Trans. Signal Process.*, vol. 64, no. 23, pp. 6174–6189, 2016.

[7] C. Wu, Y. Liu *et al.*, "Coverage characterization of STAR-RIS networks: NOMA and OMA," *IEEE Commun. Lett.*, vol. 25, no. 9, pp. 3036–3040, 2021.

[8] M. Aldababsa, A. Khaleel, and E. Basar, "Simultaneous transmitting and reflecting intelligent surfaces-empowered NOMA networks," 2021. [Online]. Available: https://arxiv.org/abs/2110.05311.

[9] C. Zhang, W. Yi *et al.*, "STAR-IOS aided NOMA networks: Channel model approximation and performance analysis," *IEEE Trans. Wireless Commun.*, 2022.

[10] X. Yue, J. Xie *et al.*, "Simultaneously transmitting and reflecting reconfigurable intelligent surface assisted NOMA networks," 2021. [Online]. Available: https://arxiv.org/abs/2112.01336.

[11] E. Björnson and L. Sanguinetti, "Rayleigh fading modeling and channel hardening for reconfigurable intelligent surfaces," *IEEE Wireless Commun. Lett.*, vol. 10, no. 4, pp. 830–834, 2020.

[12] T. Van Chien, A. K. Papazafeiropoulos *et al.*, "Outage probability analysis of IRS-assisted systems under spatially correlated channels," *IEEE Wireless Commun. Lett.*, vol. 10, no. 8, pp. 1815–1819, 2021.

[13] M.-M. Zhao, Q. Wu *et al.*, "Intelligent reflecting surface enhanced wireless networks: Two-timescale beamforming optimization," *IEEE Trans. Wireless Commun.*, vol. 20, no. 1, pp. 2–17, 2020.

[14] X. Mu, Y. Liu *et al.*, "Simultaneously transmitting and reflecting (STAR) RIS aided wireless communications," *IEEE Trans. Wireless Commun.*, Early Access, 2021.

[15] J. Xu, Y. Liu *et al.*, "STAR-RISs: Simultaneous transmitting and reflecting reconfigurable intelligent surfaces," *IEEE Commun. Lett.*, vol. 25, no. 9, pp. 3134–3138, 2021.

[16] Z. Zhang, J. Chen *et al.*, "On the secrecy design of star-ris assisted uplink noma networks," 2021. [Online]. Available: httpps://arxiv.org/abs/2111.02642.

[17] Q. Wu and R. Zhang, "Beamforming optimization for wireless network aided by intelligent reflecting surface with discrete phase shifts," *IEEE Trans. Commun.*, vol. 68, no. 3, pp. 1838–1851, 2020.

[18] T. Wang, M.-A. Badiu *et al.*, "Outage probability analysis of RIS-assisted wireless networks with Von Mises phase errors," *IEEE Wireless Commun. Lett.*, vol. 10, no. 12, pp. 2737–2741, 2021.

[19] T. Wang, G. Chen *et al.*, "Study of intelligent reflective surface assisted communications with one-bit phase adjustments," in *Proc. IEEE Global Commun. Conf. (GLOBECOM)*, Virtual, Dec. 2020, pp. 1–6.

[20] T. Wang, M.-A. Badiu *et al.*, "Performance analysis of IOS-assisted NOMA system with channel correlation and phase errors," 2021. [Online]. Available: https://arxiv.org/abs/2112.11512.

[21] J. Zhu, Y. Huang *et al.*, "Power efficient IRS-assisted NOMA," *IEEE Trans. Commun.*, vol. 69, no. 2, pp. 900–913, 2020.

[22] S. Atapattu, R. Fan *et al.*, "Reconfigurable intelligent surface assisted two–way communications: Performance analysis and optimization," *IEEE Trans. Wireless Commun.*, vol. 68, no. 10, pp. 6552–6567, 2020.

[23] E. Stauffer, O. Oyman *et al.*, "Finite-SNR diversity-multiplexing tradeoffs in fading relay channels," *IEEE J. Sel. Areas Commun.*, vol. 25, no. 2, pp. 245–257, 2007.